Wake Induced Long Range Repulsion of Aqueous Dunes

Karol A. Bacik[1,*] Sean Lovett,[2,†] Colm-cille P. Caulfield,[3,1] and Nathalie M. Vriend[1,3]

[1]*Department of Applied Mathematics & Theoretical Physics, University of Cambridge,*
Centre for Mathematical Sciences, Wilberforce Road, Cambridge CB3 0WA, United Kingdom
[2]*Schlumberger Cambridge Research, High Cross, Madingley Rd, Cambridge CB3 0EL, United Kingdom*
[3]*BP Institute, University of Cambridge, Bullard Laboratories, Madingley Road, Cambridge CB3 0EZ, United Kingdom*

Sand dunes rarely occur in isolation, but usually form vast dune fields. The large scale dynamics of these fields is hitherto poorly understood, not least due to the lack of longtime observations. Theoretical models usually abstract dunes in a field as self-propelled autonomous agents, exchanging mass, either remotely or as a consequence of collisions. In contrast to the spirit of these models, here we present experimental evidence that aqueous dunes interact over large distances without the necessity of exchanging mass. Interactions are mediated by turbulent structures forming in the wake of a dune, and lead to dune-dune repulsion, which can prevent collisions. We conjecture that a similar mechanism may be present in wind driven dunes, potentially explaining the observed robust stability of dune fields in different environments.

It is well known that sufficiently strong wind and water flow can transport sand particles. Under the action of the overlaying fluid, the particles can self organize into regular patterns. Terrestrial and extraterrestrial deserts, as well as seabeds and river bottoms, are often populated with undulating bedforms, such as dunes [1,2]. Dunes rarely occur in isolation, but usually form striking collectives known as dune fields or dune corridors. One of the reasons why the dune field landscapes are so captivating is their apparent spontaneous ordering and spatial regularity [3–5]. Nevertheless, it is an open question whether the dune configurations we observe in the field are stable or transient [4].

Because active dunes migrate, the dune fields are not stationary but translate on a slow timescale compared to the individual particle transit times. When the bedform migration rate differs between individual dunes, the dune pattern not only translates, but also evolves with time. Indeed, the migration rate is controlled by the incident flow and the dune's own size [6–8] and in a spatially heterogeneous field both of these may vary. The influence of the flow field is more subtle and not fully understood, but the relationship between the dune's size and its migration rate has been studied extensively [6–8]. There is solid empirical evidence that smaller dunes migrate faster [2,9,10], or more precisely, the migration rate is a decreasing function of the dune's mass, all else being equal. Differential speeds between individual dunes may lead to dune collisions [4,11–14]. Destructive collisions decrease the number of dunes through coalescence, in principle until one giant dune appears [4]. That scenario has not been observed in nature and one theory conjectures that the emergence of giant dunes is suppressed by "calving," i.e., the splitting of large barchan dunes [15]. Alternative explanations emphasize the role of nondestructive collisions, i.e., collisions which lead to redistribution of mass between bedforms, but conserve the number of dunes [12,16]. Empirically inferred collision rules combined with a migration rate law suffice to construct a reduced model of a dune field, with individual dunes abstracted as autonomous, self-propelled agents [4,12,15–19]. Numerical realizations of such models generate billiardlike systems in which dunes continue to collide and exchange mass until they are identical in size and thus of constant speed [12]. We present experimental results which appear to contradict this picture qualitatively. We demonstrate that the presence of an "upstream" dune can significantly affect the migration rate of a sufficiently close "downstream" dune without exchanging mass. This feedback, induced by the separation bubble and wake forming on the downstream face of dunes, generically leads to dune-dune repulsion, suppresses dune collisions, and stabilizes both homogeneous and heterogeneous dune fields.

To demonstrate this repulsion we confine attention to a two-body problem, i.e., two isolated dunes moving on a bare substrate, one directly upstream of the other. We also impose that the dunes are quasi-two-dimensional, and that there is no spanwise (i.e., in a direction orthogonal to the dominant ambient flow direction) offset between them. Bedforms of this type can be successfully realized experimentally in a narrow channel with unidirectional flow [20,21]. In our experiments, dunes are created by turbulent water flow (Re ≈ 36 000 based on dune height), directly
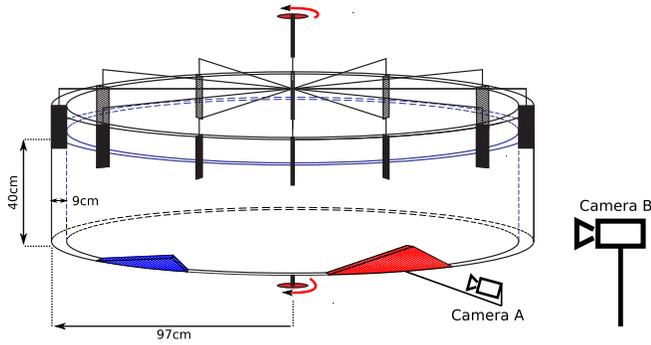
FIG. 1. The experimental apparatus. 12 equispaced paddles rotating with angular speed Ω_{paddle} drive water flow in the tank mounted on a turntable which rotates in the opposite direction at Ω_{table}. Data are collected using two camera types. Camera A corotates with the table and provides qualitative information about local sediment transport. Camera B rests in the lab frame and records the longtime evolution of the morphology. When the frame rate is increased, camera B can be also used for flow imaging. The dominant water flow is counterclockwise, and so from the upstream blue dune to the downstream red dune.

mimicking dunes forming on sea floors and river beds. We conclude with a brief discussion of which of our findings can be extrapolated to aeolian dunes [9,21,22].

To enable long-term observations we use an annular flume with radius ratio $\eta := r_i/r_o = 88 \text{ cm}/97 \text{ cm} = 0.91$, approximating an infinitely long straight channel (Fig. 1). The flume rests on a turntable and a turbulent shear flow is created by rotating paddles submerged near the free surface. The flume itself also rotates in the opposite direction, which facilitates data collection and minimizes the effects of forces induced by rotation [23]. Although secondary flows cannot be removed completely, by carefully choosing the rotation rates Ω_{table} and Ω_{paddle}, we can minimize lateral motion of the grains and create dunes that are close to quasi-two-dimensional, in the sense that the dune crest is close to horizontal and aligned in a purely radial direction.

We place two quasi-triangular piles of glass beads (diameter 1–1.3 mm), each of mass 2.25 kg, and separated by $\pi/4$ in the azimuthal coordinate of the flume. Upon initializing the motion, the flow quickly molds each pile into a characteristic dune shape with steep downstream face and shallow upstream face. To leading order, the dunes are self-contained, in that they each migrate downstream without exchanging sediment. Crucially, even though the two dunes have equal mass, their migration rate is not equal. The spacetime diagram in Fig. 2, reconstructed from an 80 min long recording with the stationary camera B (see Fig. 1), shows that the upstream dune maintains a close-to-constant speed $c_u \simeq 12.2 \text{ mh}^{-1}$. Initially, the downstream dune is significantly faster than the upstream dune (with $c_d \simeq 16.5 \text{ mh}^{-1}$), so the dunes start to separate. Eventually, the dunes converge to an antipodal configuration, with an angular separation of π. The upstream and downstream
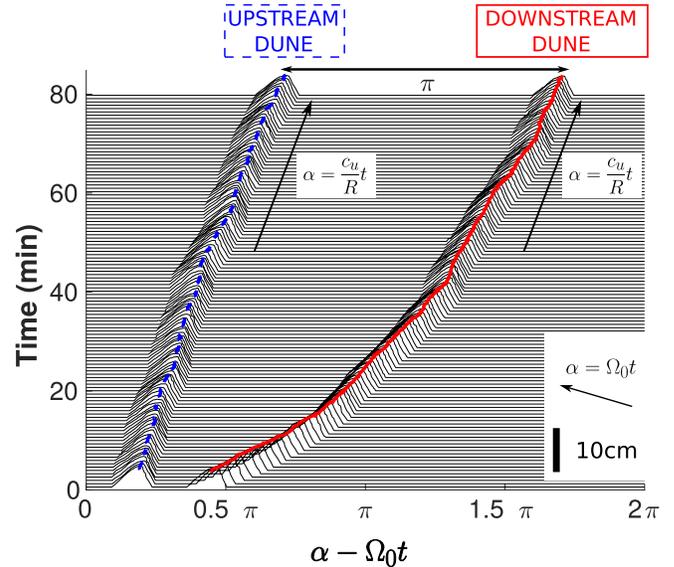

FIG. 2. Dune repulsion. Spacetime diagram in a frame of reference moving with angular speed $\Omega_0 = 1.64 \text{ h}^{-1}$. The upstream (dashed blue) dune of initial mass 2.25 kg maintains close-to-constant speed $c_u \simeq 12.2 \text{ mh}^{-1}$, while the downstream (solid red) dune (also of initial mass 2.25 kg) decelerates and converges towards $c_d \rightarrow c_u$ from above.

classification is no longer appropriate, the dune-dune interaction is symmetric, and the dunes have equal speeds. Therefore, the (maximum) interaction separation is at least as long as half of the flume's circumference, which is equivalent to approximately 60 dune heights or 6 dune lengths. In general, the interaction separation depends on the size of the dunes. We find that dunes generically initially separate from each other but sufficiently small dunes equilibrate before they attain the antipodal configuration.

The dune-dune feedback observed in this experiment is mediated by the fluid flow and is closely linked to the turbulent structures generated in the wake of the upstream dune. In fact, we can observe the signature of turbulent fluctuations in the sediment dynamics itself. At the downstream dune, the continuity of sediment flux is intermittently interrupted (and enhanced) by sudden bursts and sweeps corresponding to relatively high-speed gusts in the flow (see videos in the Supplemental Material [24]). We quantify these events with the help of a corotating camera A (see Fig. 1) mounted to the turntable. Camera A records at a frame rate of 25 Hz with long exposure time, at which the mobile layer on top of a dune appears blurred. By choosing a color threshold, we can estimate the fraction of the pixels ϕ corresponding to the mobile grains. As the migrating dune moves across the field of view, the image mobile fraction ϕ first increases until the dune fills the entire window, and subsequently decreases to zero.

Figure 3(a) shows that the size of the visible mobile layer for the downstream dune is not only larger, but also

experiences larger short-time fluctuations corresponding to the bursts in sediment flux. In order to assess the magnitude of these fluctuations we compute the running average $\bar{\phi}$ and consider the time series of

$$\Gamma = \ln \phi - \ln \bar{\phi}. \tag{1}$$

The variance of Γ, which we denote σ^2, is an approximate measure of sediment flux fluctuations. Figure 3(b) shows that magnitude of σ for the upstream dune does not change

appreciably throughout the separation, which suggests that the upstream dune experiences quasisteady flow conditions. For the downstream dune, the strength of fluctuations, as measured by σ, decreases as the dunes separate. This demonstrates that the migration rate of the downstream dune correlates well with the strength of sediment transport fluctuations.

The fluctuations of sediment transport are associated with turbulent flow structures impinging on the downstream dune. The intensity of these structures is a function of the
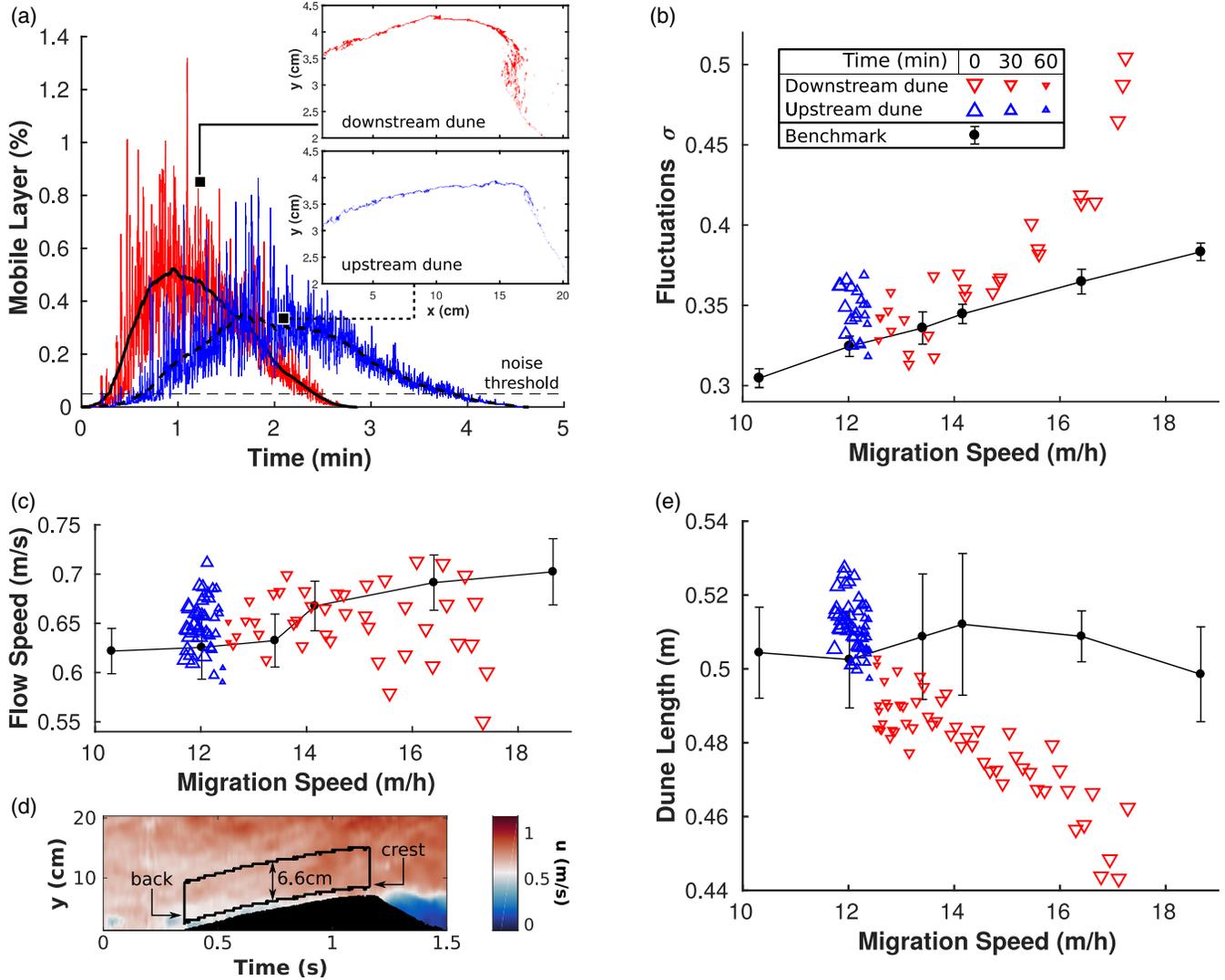

FIG. 3. (a) Time series of the image mobile fraction ϕ for the downstream (red) and the upstream (blue) dune. Dark lines (solid red and dashed blue) correspond to the running averages $\bar{\phi}$ and their shape reflects the passing of a dune through the field of view. Inset shows representative snapshots of the video footage. Colored regions correspond to the image mobile fraction ϕ. (b) Variation of fluctuation measure σ with migration speed. At early times (large symbols) when the dunes are close together, σ is significantly larger for the downstream (red down triangles) dune, due to the prevalence of bursting events, but then converges to values characteristic of the upstream (blue up triangles) dune. Black line benchmarks correspond to isolated dunes of the same mass subjected to variable flow conditions at different rotation rates of the paddle (c) Variation of instantaneous azimuthal flow speed (averaged near the dune) with migration speed for both dunes, suggesting that the mean flow speed over the downstream dune does not change significantly with migration speed and hence separation. (d) The black box denotes the averaging region for the reference flow speed in panel (c). It is fitted to the dune and stretches from 1 to 7.6 cm above its surface. (e) Variation of dune length with migration speed, demonstrating that the downstream dune elongates as it separates (and decelerates), while the upstream dune demonstrates smaller and uncorrelated length variation.

proximity of the upstream dune. Indeed, the values of σ for the downstream dune are substantially larger when compared to the benchmark dunes, i.e., single isolated dunes. Moreover, the strength of fluctuations decays as the dunes separate, which agrees with the expectation that turbulent perturbations decay as they are advected away from their source, i.e., away from the upstream dune.

The abundant production of turbulence in a dune's wake is not entirely surprising. Various turbulent mechanisms associated with a dune's wake, for example, rolls, sweeps, or bursts, have been identified and classified in previous studies [22,25–27]. We conjecture that the turbulence intensity in fact controls the dune migration rate. In a simple migration speed model [1,2], where sediment reacts instantaneously to changes in shear stress, velocity fluctuations make a positive contribution to the migration speed. Indeed, the migration speed of self-contained dunes is directly controlled by the time-integrated sediment flux q, which is a strictly convex function of the shear velocity u^* [28,29]. At high Reynolds numbers u^* can be linearly related to the true fluid velocity field at a fixed distance above the surface, and thus it is often argued that the shear stress is proportional to some quadratic function of appropriate velocities [1,29,30]. Whatever the particular functional form, convexity of $q(u^*)$ is sufficient to imply that for a fixed mean velocity field, increasing the amplitude of the fluctuations necessarily increases the time integral of q. Experiments also confirm that turbulent fluctuations can strongly increase sediment flux even if the mean velocity is unchanged [31,32].

Unfortunately, curvature and rotation hinder precise flow imaging in our experiment. Nevertheless, crude velocity measurements utilizing particle tracking [33] suggest that the mean flow velocity indeed does not differ between the two separating dunes. The reference flow speed plotted in Fig. 3(c) is defined as an instantaneous azimuthal velocity averaged over a large dune-fitted region [see Fig. 3(d)]. Qualitatively, the results of this coarse measure are in agreement with more precise experiments [22,27] and direct numerical simulations [25,26] which all suggest that the mean flow velocity is not higher at the downstream dune. Furthermore, the intensity of the wake-induced turbulence naturally decreases as the dune-dune separation increases [34]. Therefore sufficiently large dunes (with sufficiently vigorous wakes) will naturally equilibrate to an antipodal configuration. In summary, we conclude that it is highly plausible that the velocity fluctuations themselves enhance sediment flux and thus cause the observed dune-dune repulsion. We should also point out that while the bursts in our experiment do not have any apparent chirality, the significance of secondary across-channel circulation and streamwise vortices, specific to our rotating setup, is yet to be determined.

Elevated turbulence also affects the shape of the downstream dune, which to first approximation can be characterized by dune height and length. Initially, the

downstream dune has greater height and smaller length compared to the upstream dune and as it "escapes" it relaxes towards a more elongated shape [see Fig. 3(d) and insets of Fig. 3(a)]. Figure 3(e) also shows that the length of the downstream dune does not converge precisely to the length of the upstream dune. This offset is a signature of a small mass redistribution which is another consequence of the flow asymmetry. Enhanced turbulent bursts cause relatively more particles to bypass the separation bubble that traps most of the particles and leave the downstream dune. After leaving the dune, such grains roll or slide over the bare substrate and, due to the periodic geometry, accumulate at the other dune. As a result, in the course of separation, the downstream dune loses approximately 3% mass (as measured directly after the experiment). We should emphasize however, that the mass difference is a consequence rather than a cause of the dune repulsion. In a periodic domain the particles that leave the downstream dune accumulate at the upstream dune (making it slightly larger), but in a longer train of bedforms they would be incorporated into the next dune downstream. For simplicity and clarity, we have focused exclusively on dunes propagating over a solid substrate. Additional effects may ensue if the dunes interact with an underlying layer of erodible sediment. Transport into and out of such a layer may lead to further asymmetric behavior between upstream and downstream dunes. In three dimensions, sediment exchange dynamics can be even more complex as barchan dunes lose sand preferentially through their horns at the downstream end [4].

Dune-dune repulsion due to wake-induced enhanced sediment flux stabilizes dune field configurations as it prevents collisions even if the dunes are of different sizes. Figure 4 shows two dunes differing in mass by a factor of
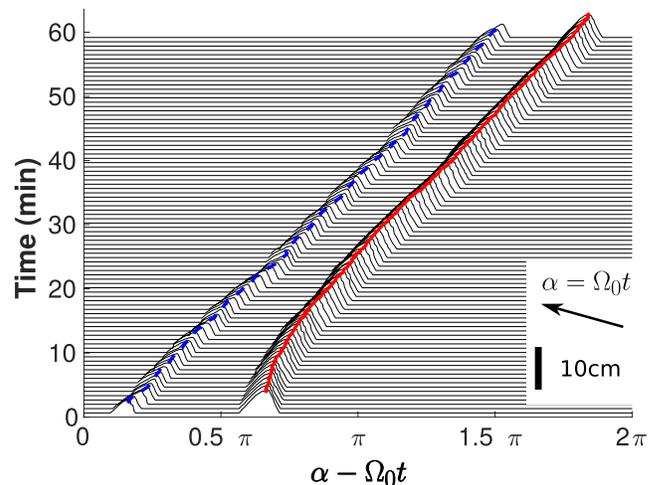

FIG. 4. Collision suppression. Spacetime diagram in a frame of reference moving with angular speed $\Omega_0 = 2.46 \text{ h}^{-1}$. After initial repulsion, the downstream dune of initial mass 2.25 kg (red solid) migrates at the same rate as the upstream dune of initial mass 0.9 kg (blue dashed).

2.5, which are initially positioned at an angular separation of $\pi/2$. Initially, the relatively small upstream dune migrates faster, but as the separation distance decreases, the wake-induced repulsion grows stronger, and the relatively large downstream dune speeds up. Eventually, the repulsion effect balances the tendency of larger dunes to migrate more slowly, and the two dunes migrate at the same rate even though they have markedly different sizes. This leads to a metastable configuration which, on a significantly slow timescale, is destabilized by the relative loss of mass by the downstream dune.

Within our experiment dune-dune repulsion is a very robust phenomenon. If dunes are sufficiently close to each other, dune separation occurs for all flow regimes accessible within our apparatus. The repulsion mechanism we have studied is reminiscent of the fragmentation and splitting phenomena of 3D barchan dunes, which have been observed in other aqueous experiments [13,14,35]. These studies focused on dunes of different sizes so the interaction appears to stay short range (cf. Fig. 4). However, we speculate that when neighboring dunes are comparable in size, long-range dune-dune repulsion can be observed for fully 3D dunes as well. We conclude therefore that it is plausible that the structure of natural underwater dune fields is controlled and stabilized by the same dune-dune repulsion mechanism observed in this work.

For aeolian dunes, the dune-based Reynolds numbers are higher than in our experiment, so turbulent wakes are likely to form behind such dunes as well. At the same time, the momentum carried by flow within the wake is relatively lower, and the particle-fluid density ratio is higher, so it is *a priori* unclear whether turbulence has the same impact on sediment transport. Nevertheless, it is still definitely plausible that wake-induced turbulent bursts and sweeps will still enhance sediment flux relatively on downstream dunes, and also that such enhancement increases as the distance to upstream dunes decreases [34]. Indeed, there are satellite images that suggest that repulsion can be also observed in deserts [e.g., Fig. 2 of Ref. [36] or Fig. 1(b) of Ref. [14]]. These observations show repulsive interactions between dunes of different sizes, analogous to our Fig. 4. Thus, it appears that the repulsion may play a role in shaping aeolian sedimentary landscapes as well. Nevertheless, in geological cases, the complexity of dune-dune interactions can increase due to sediment flux between dunes [4], transverse diffusion of sediment [37,38], and 3D effects [13,14,22].

*kab81@cam.ac.uk
†Present address: Invenia Labs, 95 Regent Street, Cambridge CB2 1AW, United Kingdom.

[1] B. Andreotti, Y. Forterre, and O. Pouliquen, *Granular Media* (Cambridge University Press, Cambridge, England, 2013).

[2] F. Charru, B. Andreotti, and P. Claudin, Annu. Rev. Fluid Mech. **45**, 469 (2013).

[3] B. Andreotti, P. Claudin, and S. Douady, Eur. Phys. J. B **28**, 341 (2002).

[4] P. Hersen, K. H. Andersen, H. Elbelrhiti, B. Andreotti, P. Claudin, and S. Douady, Phys. Rev. E **69**, 011304 (2004).

[5] G. Kocurek and R. C. Ewing, Geomorphology **72**, 94 (2005).

[6] K. Kroy, G. Sauermann, and H. J. Herrmann, Phys. Rev. Lett. **88**, 054301 (2002).

[7] K. Kroy, G. Sauermann, and H. J. Herrmann, Phys. Rev. E **66**, 031302 (2002).

[8] B. Andreotti, P. Claudin, and S. Douady, Eur. Phys. J. B **28**, 321 (2002).

[9] P. Hersen, S. Douady, and B. Andreotti, Phys. Rev. Lett. **89**, 264301 (2002).

[10] E. M. Franklin and F. Charru, J. Fluid Mech. **675**, 199 (2011).

[11] G. Kocurek, R. Ewing, and D. Mohrig, Earth Surf. Processes Landforms **35**, 51 (2010).

[12] M. Génois, S. C. du Pont, P. Hersen, and G. Grégoire, Geophys. Res. Lett. **40**, 3909 (2013).

[13] N. Endo, K. Taniguchi, and A. Katsuki, Geophys. Res. Lett. **31**, L12503 (2004).

[14] P. Hersen and S. Douady, Geophys. Res. Lett. **32**, L21403 (2005).

[15] S. L. Worman, A. B. Murray, R. Littlewood, B. Andreotti, and P. Claudin, Geology **41**, 1059 (2013).

[16] S. Diniega, K. Glasner, and S. Byrne, Geomorphology **121**, 55 (2009).

[17] A. R. Lima, G. Sauermann, H. J. Herrmann, and K. Kroy, Physica (Amsterdam) **310A**, 487 (2002).

[18] E. Eastwood, J. Nield, A. Baas, and G. Kocurek, Sedimentology **58**, 1391 (2011).

[19] O. Durán, V. Schwämmle, P. G. Lind, and H. J. Herrmann, Nonlinear Processes Geophys. **18**, 455 (2011).

[20] C. Groh, A. Wierschem, N. Aksel, I. Rehberg, and C. A. Kruelle, Phys. Rev. E **78**, 021304 (2008).

[21] A. Betat, V. Frette, and I. Rehberg, Phys. Rev. Lett. **83**, 88 (1999).

[22] N. Bristow, G. Blois, J. Best, and K. T. Christensen, J. Geophys. Res. **123**, 2157 (2018).

[23] A. W. Baar, J. de Smit, W. S. J. Uijttewaal, and M. G. Kleinhans, Water Resour. Res. **54**, 19 (2018).

[24] See Supplemental Material at http://link.aps.org/supplemental/10.1103/PhysRevLett.124.054501 for both raw and postprocessed footage.

[25] T. Stoesser, C. Braun, M. García-Villalba, and W. Rodi, J. Hydraul. Eng. **134**, 42 (2008).

[26] W. Anderson and M. Chamecki, Phys. Rev. E **89**, 013005 (2014).

[27] J. A. Palmer, R. Mejia-Alvarez, J. L. Best, and K. T. Christensen, Exp. Fluids **52**, 809 (2012).

[28] D. J. Sherman, D. W. T. Jackson, S. L. Namikas, and J. Wang, Geomorphology **22**, 113 (1998).

[29] J. F. Kok, E. J. R. Parteli, T. I. Michaels, and D. B. Karam, Rep. Prog. Phys. **75**, 106901 (2012).

[30] F. Charru and P. Luchini, Phys. Rev. Fluids **4**, 034304 (2019).

[31] J. M. Nelson, R. L. Shreve, S. R. McLean, and T. G. Drake, Water Resour. Res. **31**, 2071 (1995).

[32] B. M. Sumer, L. H. Chua, N. S. Cheng, and J. Fredsøe, J. Hydraul. Eng. **129**, 585 (2003).

[33] S. B. Dalziel, Appl. Sci. Res. **49**, 217 (1992).

[34] N. R. Bristow, G. Blois, J. L. Best, and K. T. Christensen, J. Geophys. Res. **124**, 1175 (2019).

[35] A. Katsuki, M. Kikuchi, H. Nishimori, N. Endo, and K. Taniguchi, Earth Surf. Processes Landforms **36**, 372 (2011).

[36] P. Vermeesch, Geophys. Res. Lett. **38**, L22402 (2011).

[37] C. A. Alvarez and E. M. Franklin, Phys. Rev. Lett. **121**, 164503 (2018).

[38] G. Seizilles, E. Lajeunesse, O. Devauchelle, and M. Bak, Phys. Fluids **26**, 013302 (2014).